Supplement of Biogeosciences, 22, 791–807, 2025
https://doi.org/10.5194/bg-22-791-2025-supplement

Biogeosciences Open Access EGU

Supplement of

What controls planktic foraminiferal calcification?

Ruby Barrett et al.

Correspondence to: Ruby Barrett (ruby.barrett@bristol.ac.uk)

Contents of this file

S1. Article list for SNW data used in Bayesian models

A) Group-level model

Barker, S.: Planktonic foraminiferal proxies for temperature and pCO2, Ph.D. thesis, University of Cambridge, England, 2002.

Béjard, T. M., Rigual-Hernández, A. S., Flores, J. A., Tarruella, J. P., Durrieu De Madron, X., Cacho, I., Haghipour, N., Hunter, A., and Sierro, F. J.: Calcification response of planktic foraminifera to environmental change in the western Mediterranean Sea during the industrial era, Biogeosciences, 20, 1505–1528, https://doi.org/10.5194/BG-20-1505-2023, 2023.

Marr, J. P., Baker, J. A., Carter, L., Allan, A. S. R., Dunbar, G. B., and Bostock, H. C.: Ecological and temperature controls on Mg/Ca ratios of Globigerina bulloides from the southwest Pacific Ocean, Paleoceanography, 26, https://doi.org/10.1029/2010PA002059, 2011.

Pallacks, S., Ziveri, P., Schiebel, R., Vonhof, H., Rae, J. W. B., Littley, E., Garcia-Orellana, J., Langer, G., Grelaud, M., and Martrat, B.: Anthropogenic acidification of surface waters drives decreased biogenic calcification in the Mediterranean Sea, Commun. Earth Environ., 4, 1–10, https://doi.org/10.1038/s43247-023-00947-7, 2023.

Barrett, R.: Planktic foraminifera size-normalised weight data and associated environmental data [dataset bundled publication]., https://doi.org/https://doi.org/10.1594/PANGAEA.973256, 2025.

B) Species-level modelling

Barker, S.: Planktonic foraminiferal proxies for temperature and pCO2, Ph.D. thesis, University of Cambridge, England, 2002.

Béjard, T. M., Rigual-Hernández, A. S., Flores, J. A., Tarruella, J. P., Durrieu De Madron, X., Cacho, I., Haghipour, N., Hunter, A., and Sierro, F. J.: Calcification response of planktic foraminifera to environmental change in the western Mediterranean Sea during the industrial era, Biogeosciences, 20, 1505–1528, https://doi.org/10.5194/BG-20-1505-2023, 2023.

Marr, J. P., Baker, J. A., Carter, L., Allan, A. S. R., Dunbar, G. B., and Bostock, H. C.: Ecological and temperature controls on Mg/Ca ratios of Globigerina bulloides from the southwest Pacific Ocean, Paleoceanography, 26, https://doi.org/10.1029/2010PA002059, 2011.

Marshall, B. J., Thunell, R. C., Henehan, M. J., Astor, Y., and Wejnert, K. E.: Planktonic foraminiferal area density as a proxy for carbonate ion concentration: A calibration study using the Cariaco Basin ocean time series, Paleoceanography, 28, 363–376, https://doi.org/10.1002/palo.20034, 2013

Pallacks, S., Ziveri, P., Schiebel, R., Vonhof, H., Rae, J. W. B., Littley, E., Garcia-Orellana, J., Langer, G., Grelaud, M., and Martrat, B.: Anthropogenic acidification of surface waters drives decreased biogenic calcification in the Mediterranean Sea, Commun. Earth Environ., 4, 1–10, https://doi.org/10.1038/s43247-023-00947-7, 2023.

Qin, B., Li, T., Xiong, Z., Algeo, T. J., and Chang, F.: Deepwater carbonate ion concentrations in the western tropical Pacific since 250 ka: Evidence for oceanic carbon storage and global climate influence, Paleoceanography, 32, 351–370, https://doi.org/10.1002/2016PA003039, 2017.

Weinkauf, M. F. G., Kunze, J. G., Waniek, J. J., and Kučera, M.: Seasonal Variation in Shell Calcification of Planktonic Foraminifera in the NE Atlantic Reveals Species-Specific Response to Temperature, Productivity, and Optimum Growth Conditions, PLoS One, 11, e0148363, https://doi.org/10.1371/journal.pone.0148363, 2016

Barrett, R.: Planktic foraminifera size-normalised weight data and associated environmental data [dataset bundled publication]., https://doi.org/https://doi.org/10.1594/PANGAEA.973256, 2025.

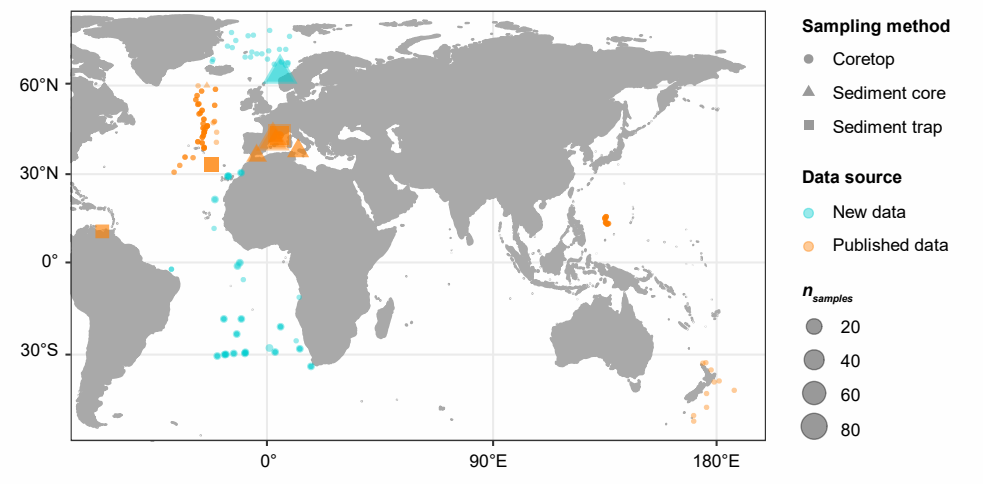

Figure S1. Location of SNW data, sampling method and number of samples per site.

G. bulloides

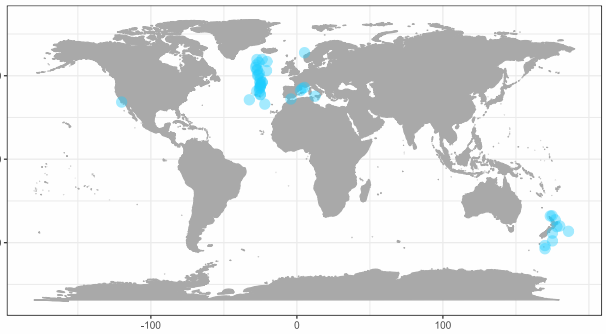

G. elongatus

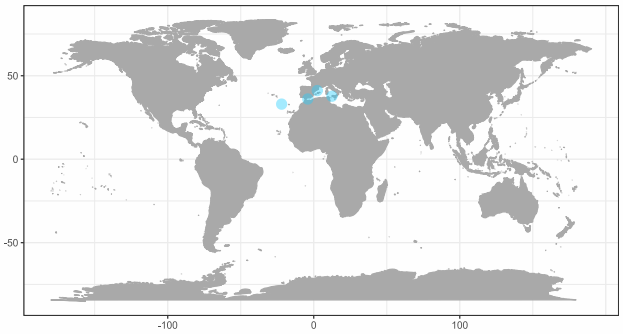

G. inflata

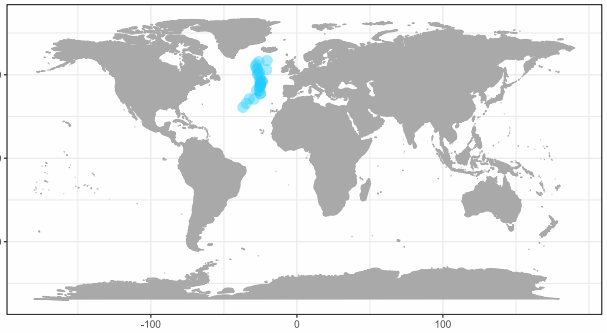

G. ruber

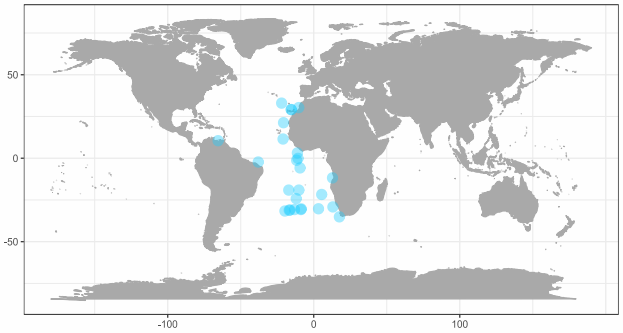

G. truncatulinoides

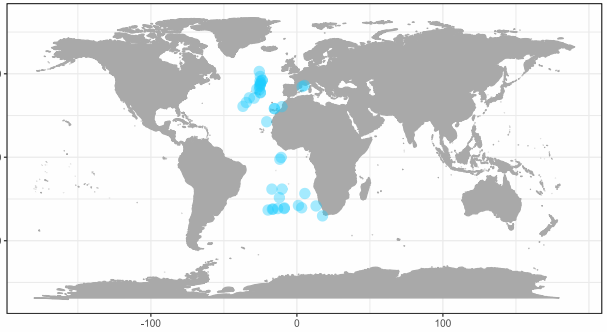

N. pachyderma

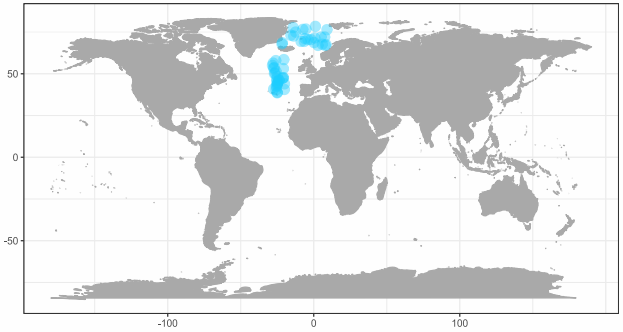

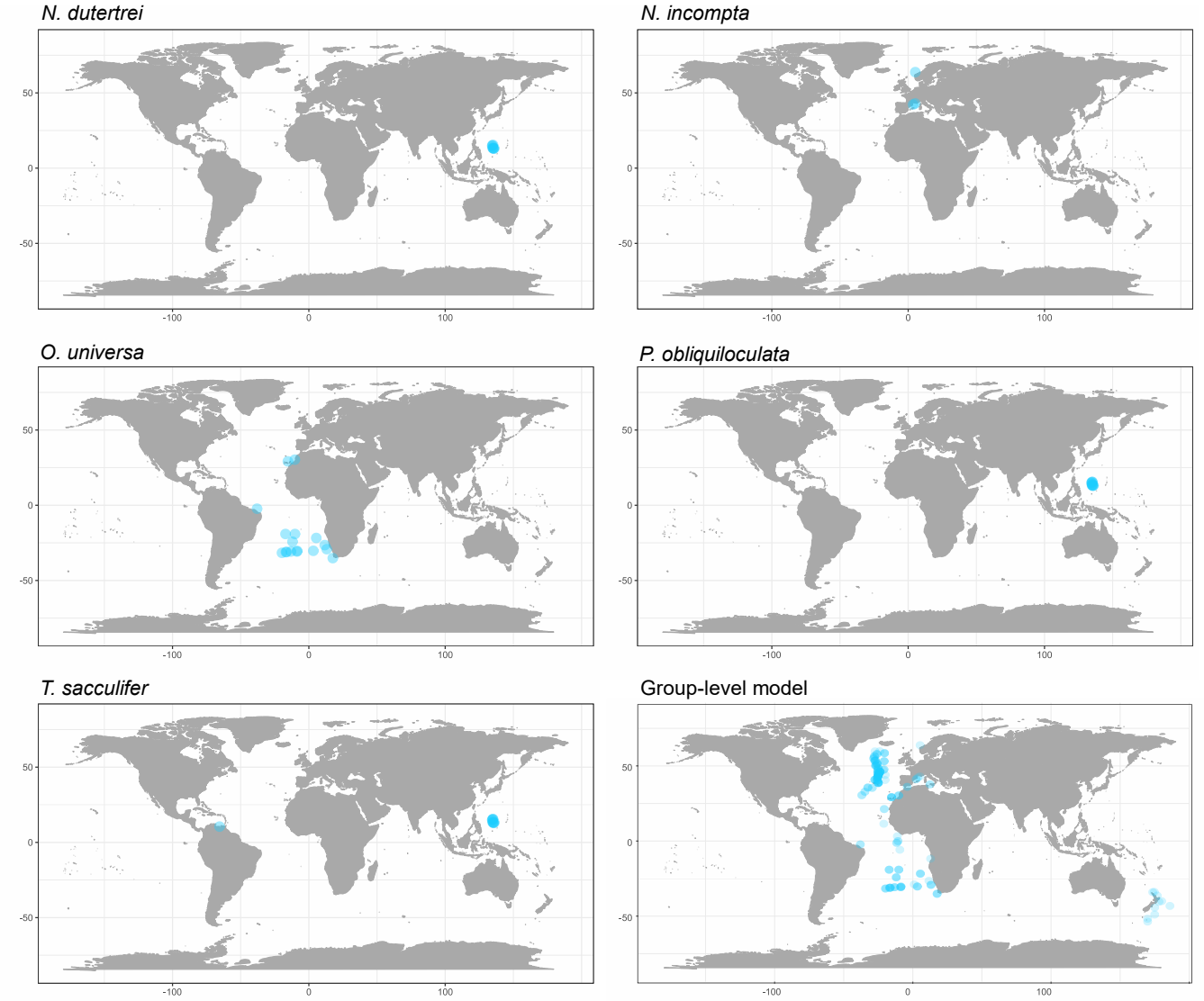

Figure S2. Location of SNW data for individual species, and locations for all SNW data included in the group-level SNW model. Data excludes plankton tow and only include SNW which are measurement based. For the group-level model, data is from a small size fraction range (250-350 µm).

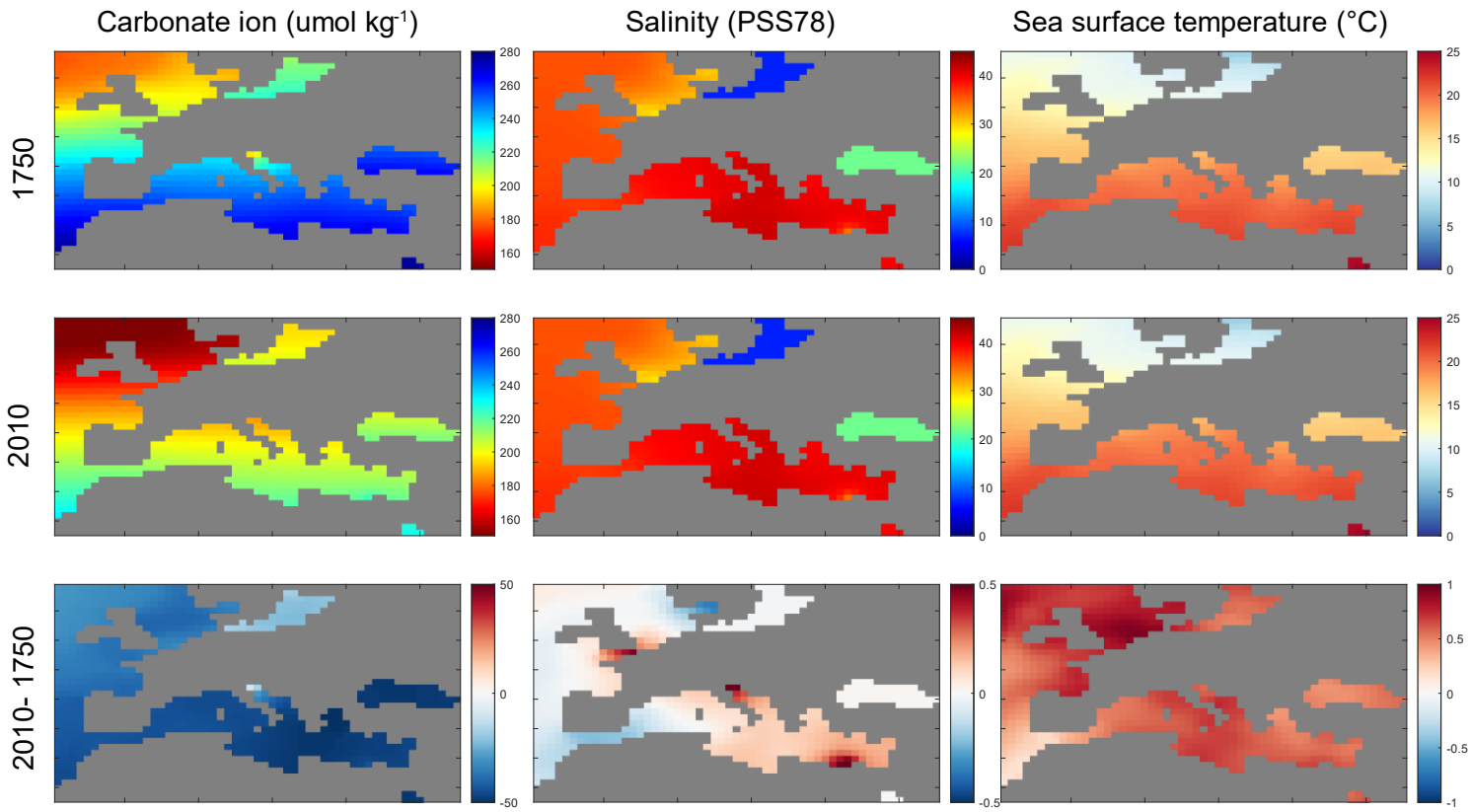

Figure S3. Mediterranean carbonate ion concentration, sea surface salinity and sea surface temperature outputs for the preindustrial (1750; preindustrial values were assumed the same as in 1850, which is average of 1850:1854) and modern (2010; average of 2005-2014), and the difference between these two time periods. Outputs are from CESM2 in the CMIP6 suite and are corrected for model drift and to GLODAP observational data, following the methods in Jiang et al. (2023). These model outputs have been manipulated to calculate decadal averages and units converted using density functions found in Table S1 and the International Thermodynamic Equation of Seawater - 2010 (TEOS-10; McDougall & Barker, 2011). Carbonate ion concentration is calculated from dissolved inorganic carbon (DIC) and alkalinity using CO2SYS (van Heuven et al., 2011).

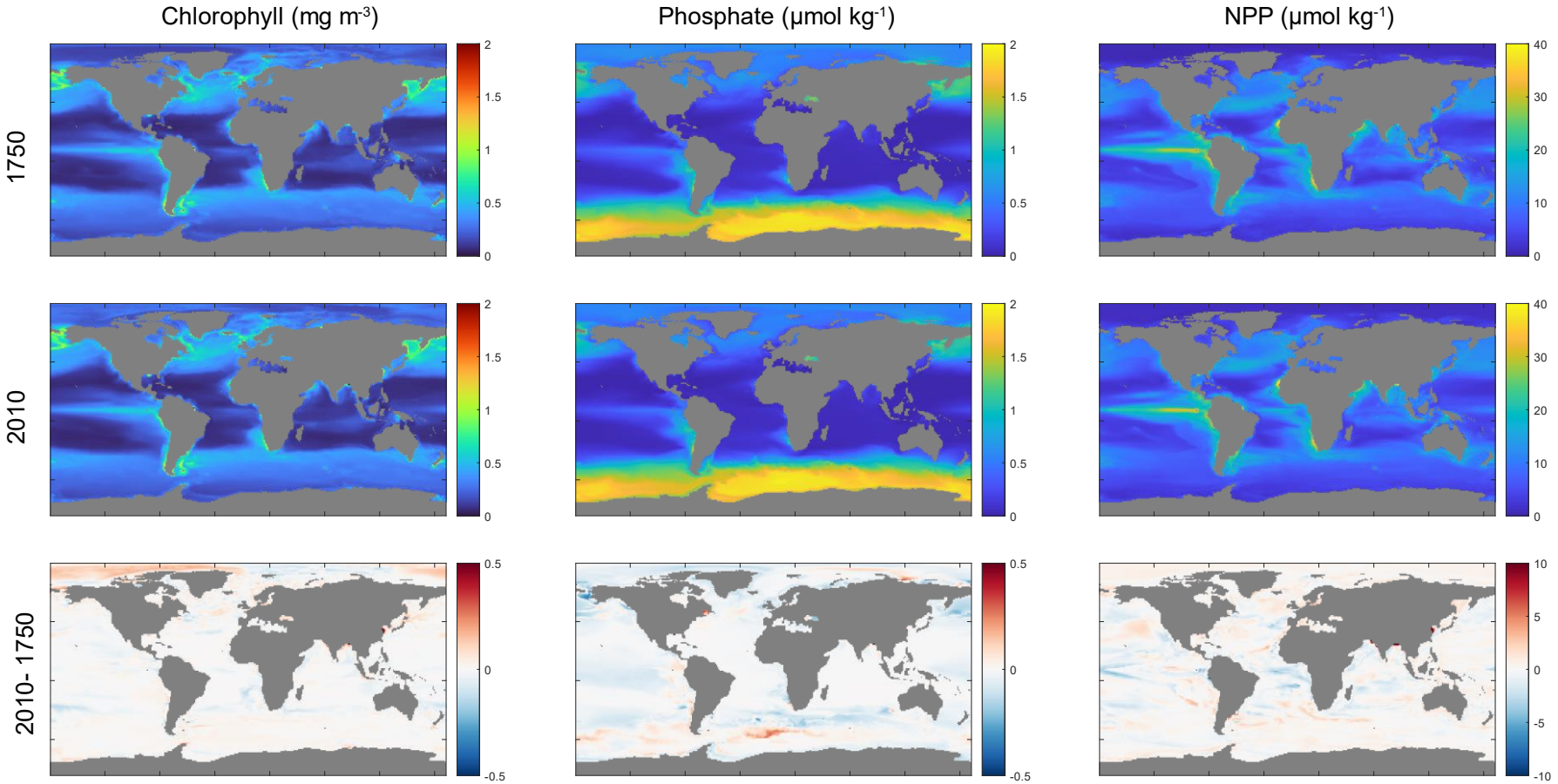

Figure S4. Chlorophyll, phosphate and NPP model outputs for the preindustrial (1750; preindustrial values were assumed the same as in 1850, which is average of 1850:1854) and modern (2010; average of 2005-2014), and difference between these time periods. Outputs are the median of CESM2, MRI ESM2, GDFL CM4, MIROC, and GFDL ESM4 from the CMIP6 suite. These data were not corrected for model drift, or to observational data as the observational data coverage is insufficient and DIVA gridding produces spurious results. Note that these model outputs have been manipulated to calculate decadal averages and units converted using density functions found in Table S1 and the International Thermodynamic Equation of Seawater – 2010 (TEOS-10; McDougall & Barker, 2011).

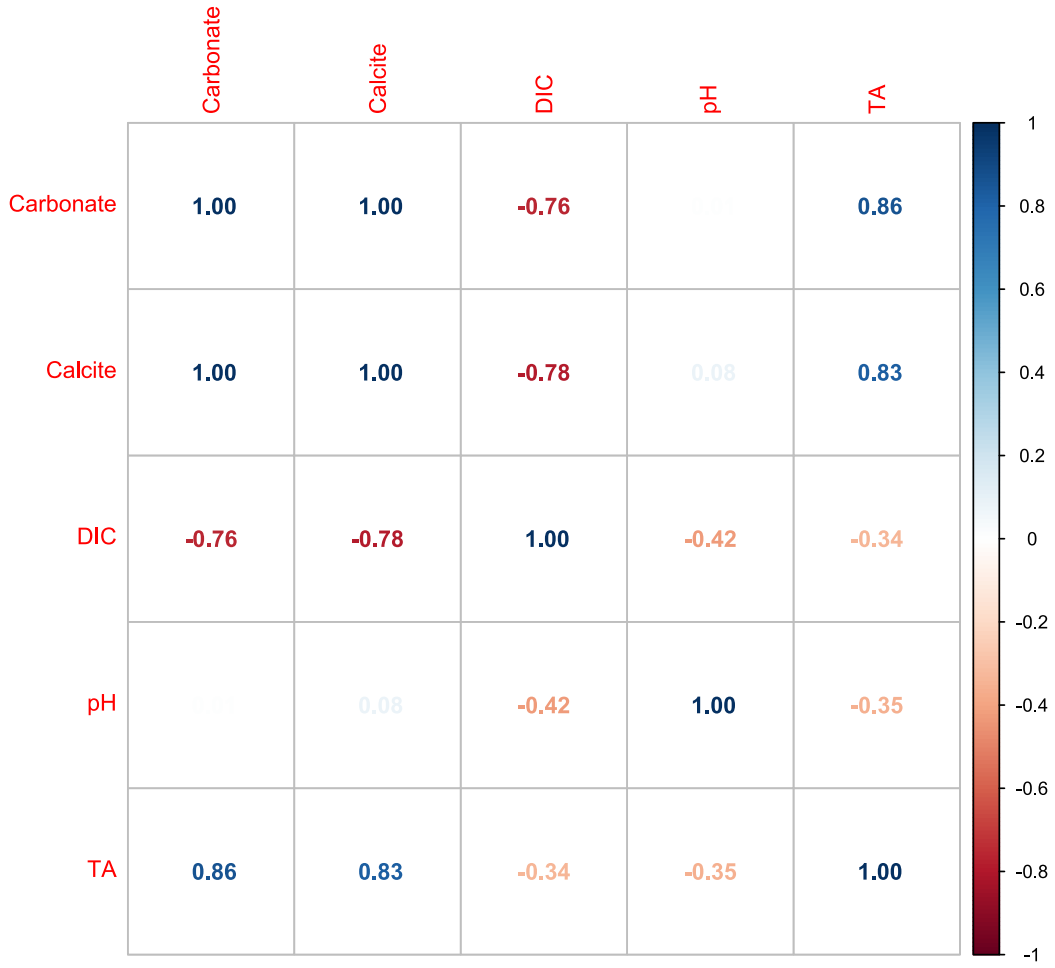

Figure S5. Spearman's output showing the high degree of correlation ($\rho > 0.7$) in the carbonate system, hence why only carbonate ion concentration was selected to represent the carbonate system.

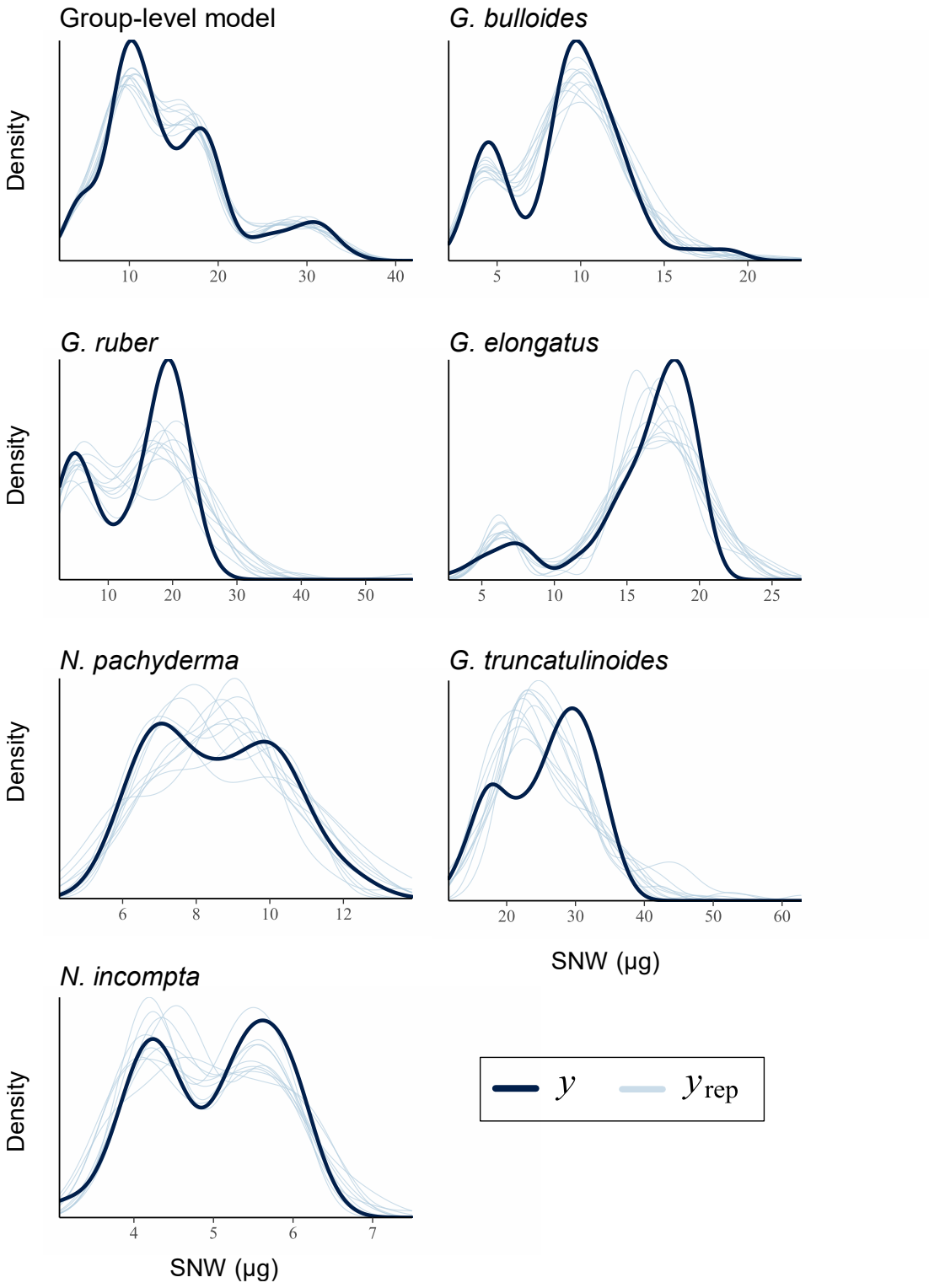

Figure S6. Kernel density estimate of the observed dataset "y", with density estimates for 100 simulated datasets "y_{rep}" drawn from the posterior predictive distribution showing goodness of fit of SNW for the Bayesian models, plotted using the pp_check function from the brms package. The closer that "y_{rep}" is to "y" means the better the model was able to reproduce the original data distribution. All models have a reasonable fit.

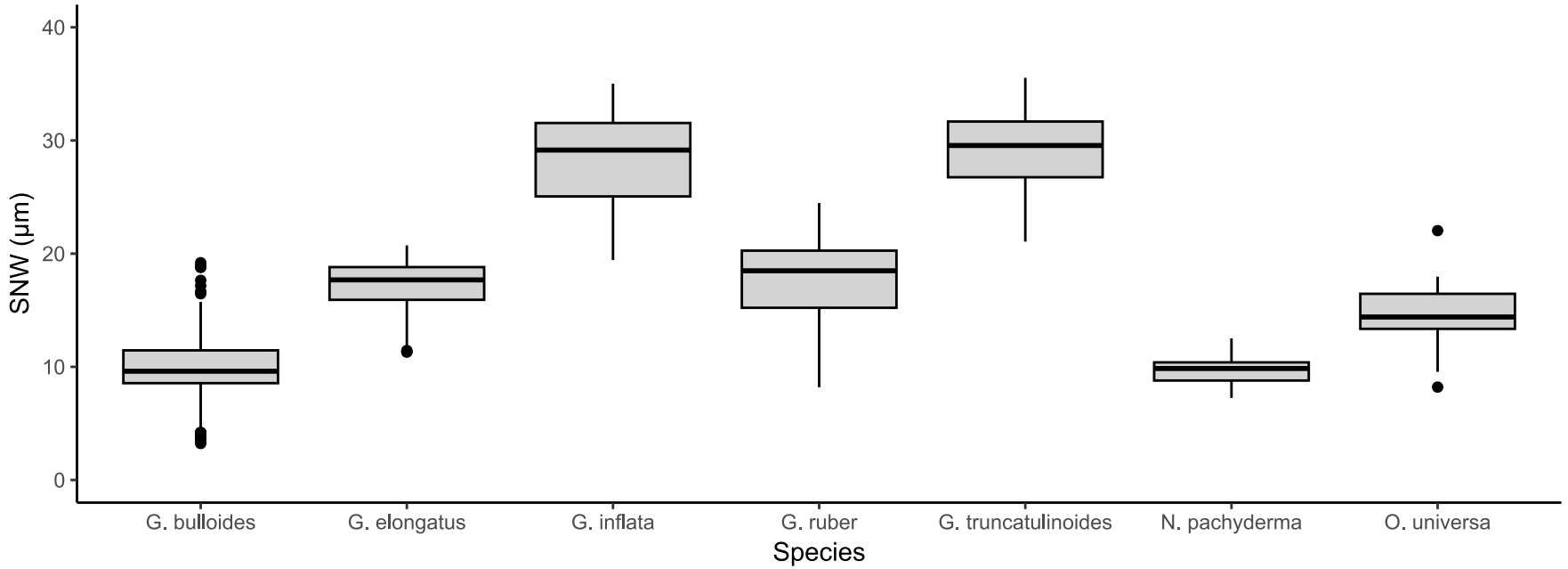

Figure S7. Size-normalised weight (SNW) of foraminiferal species used in Group-level modelling (sieved from 250-350 µm size fraction). The boxplots show the range of variance in SNW between species is unequal ("heteroscedastic"). We account for this heteroscedasticity in group-level model by adding a shape term which allows the variance between each species to vary.

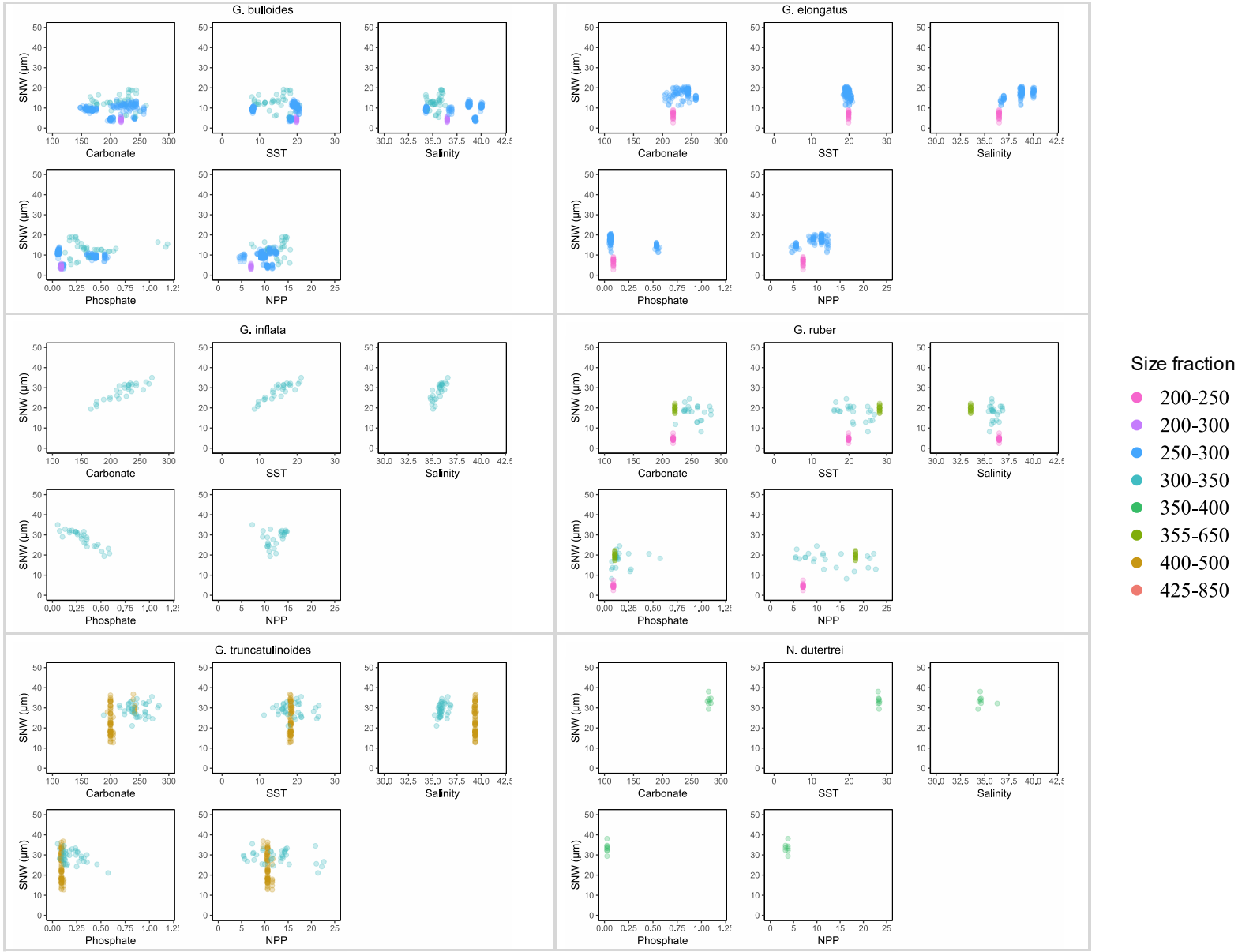
G. bulloides
G. elongatus
G. inflata
G. ruber
G. truncatulinoides
N. dutertrei
SNW (µm)
Carbonate
SST
Salinity
Phosphate
NPP
Size fraction
200-250
200-300
250-300
300-350
350-400
355-650
400-500
425-850

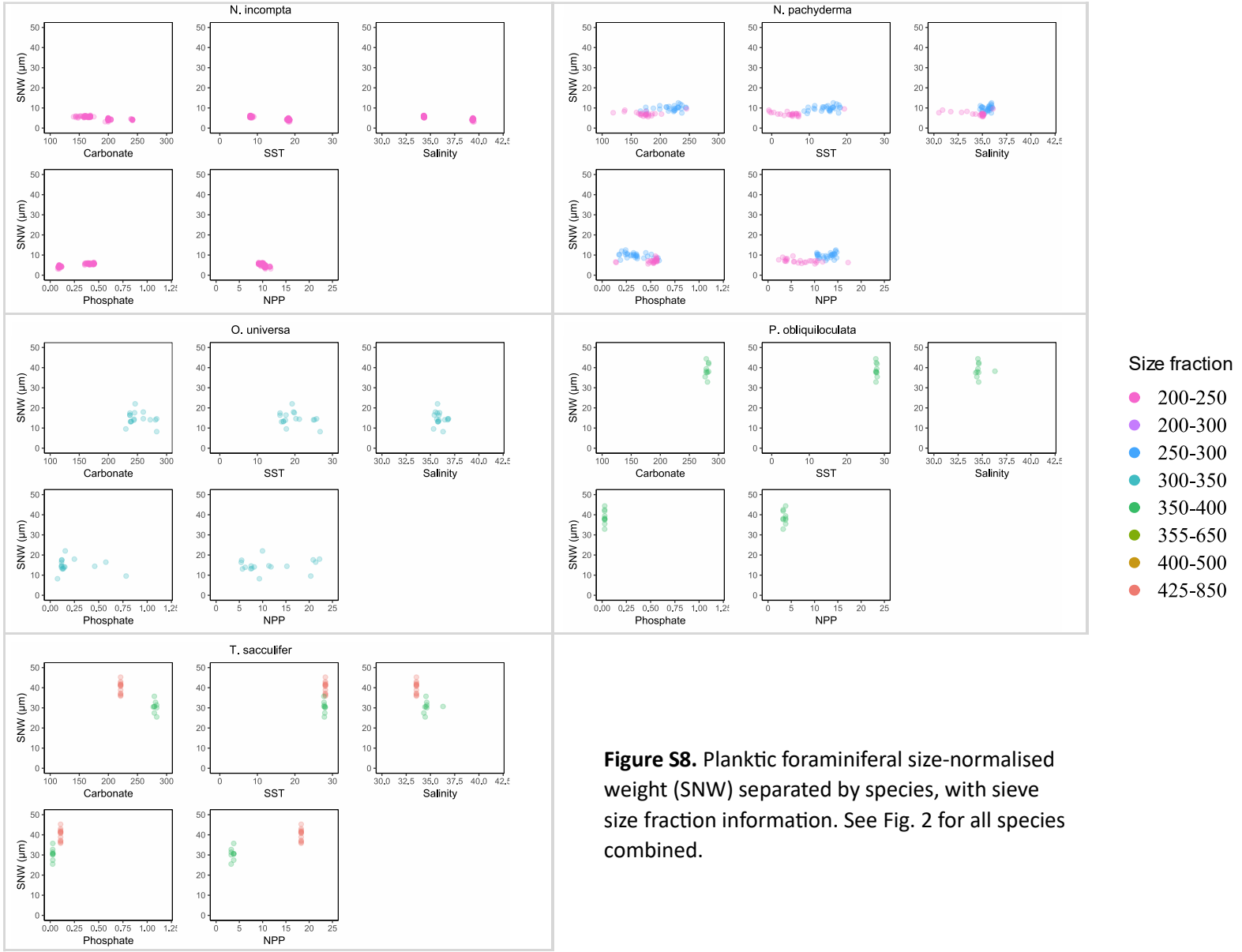

Figure S8. Planktic foraminiferal size-normalised weight (SNW) separated by species, with sieve size fraction information. See Fig. 2 for all species combined.

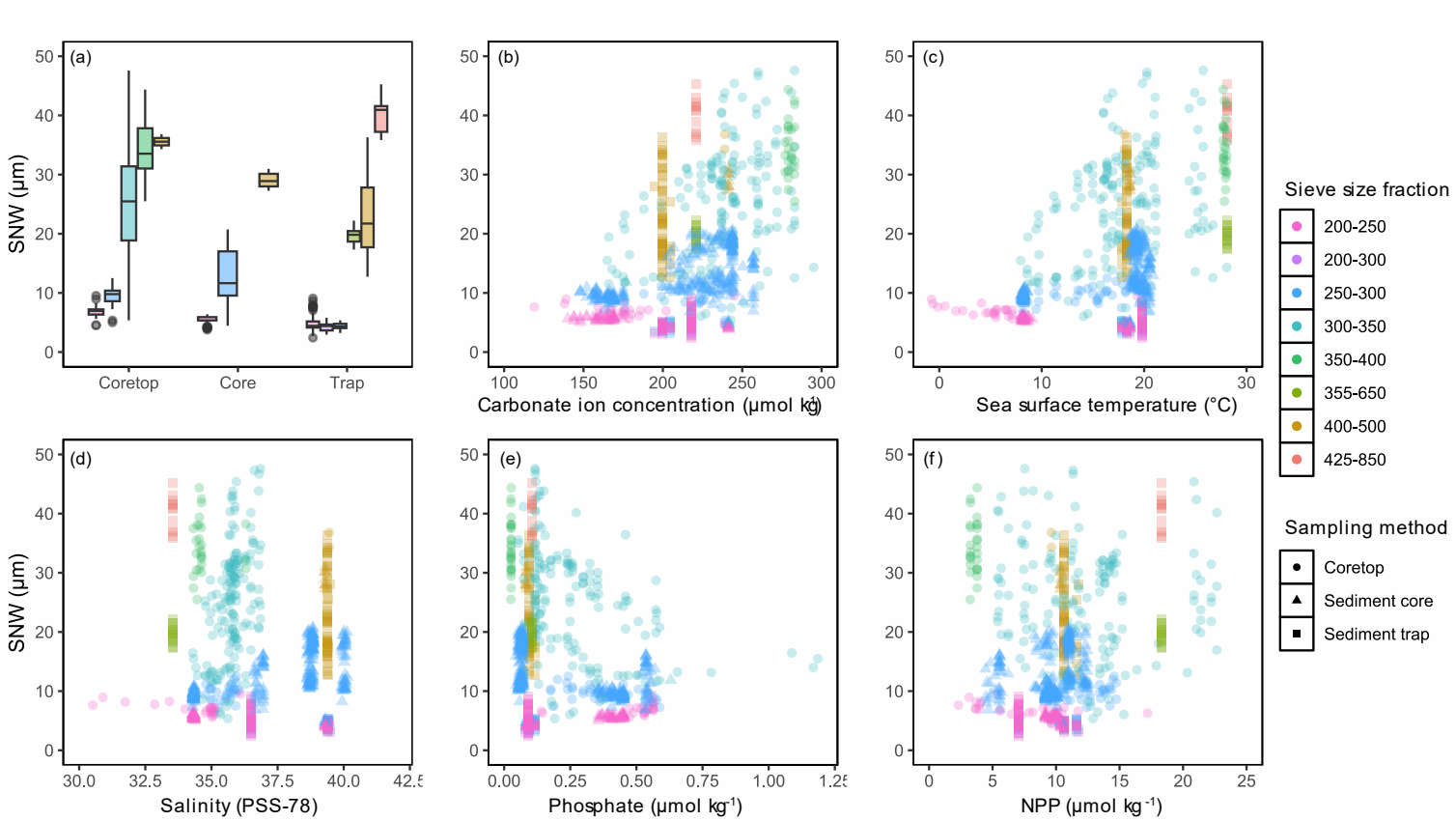

Figure S9 (a) Boxplot showing SNW distribution across sieve size fractions for different data types. (b-f) Planktic foraminiferal size-normalised weight (MBW) against environmental variables extracted from the CMIP6 modelling suite (see methods). Colour indicates the size-fraction foraminifers were initially sieved at before being normalised to their length or area.

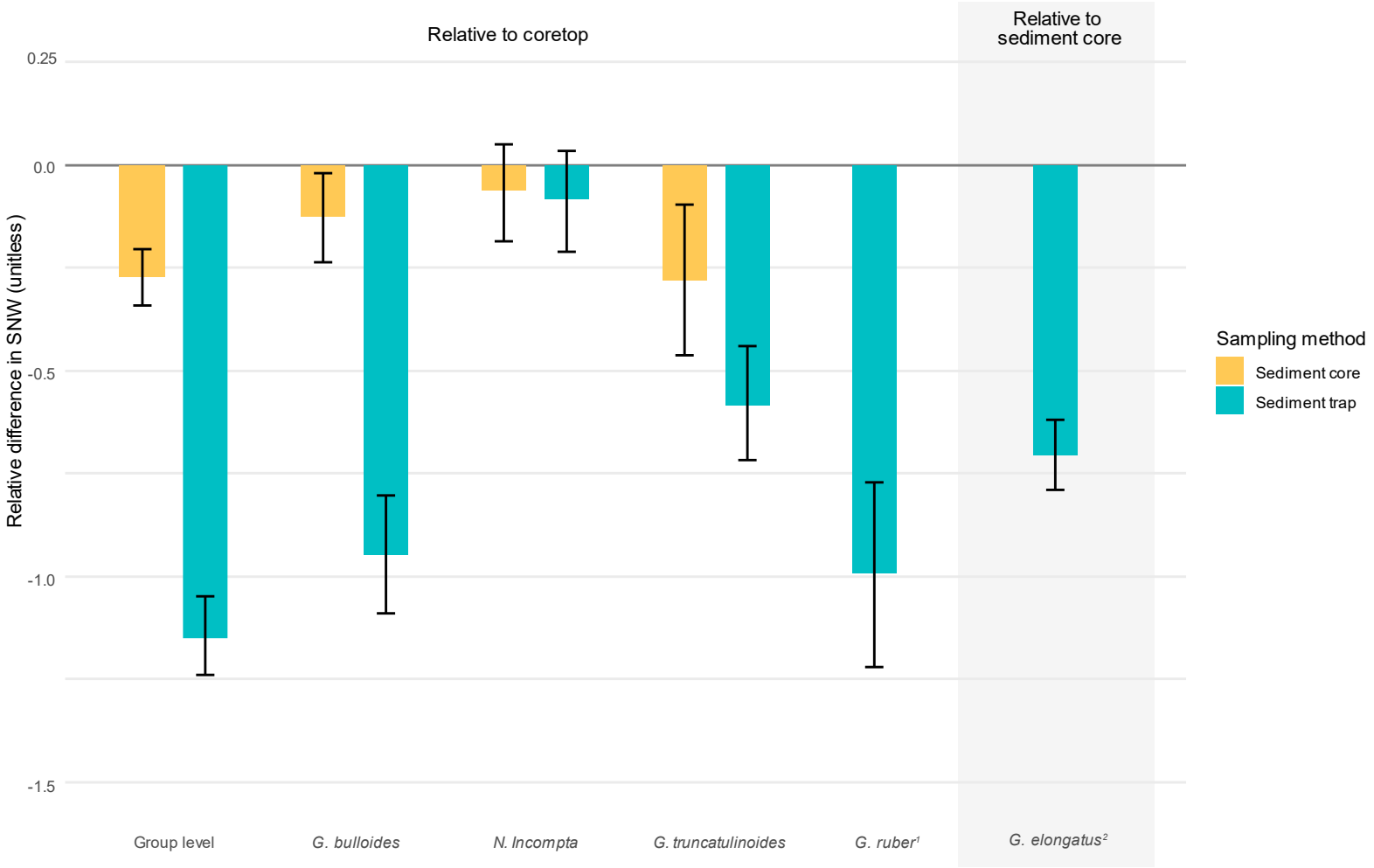

Figure S10 Bayesian model outputs showing the median difference in SNW from different sampling methods, relative to coretop data (unless stated otherwise). The more negative the value, the lighter the SNW. Black capped lines represent the 95% probability interval. *N pachyderma* is not present because this dataset contained only one sampling method (Coretop). [1] *G. ruber* does not contain any samples from sediment core data. [2] *G. elongatus* does not contain any coretop data, and the sediment trap data presented is relative to sediment core data.

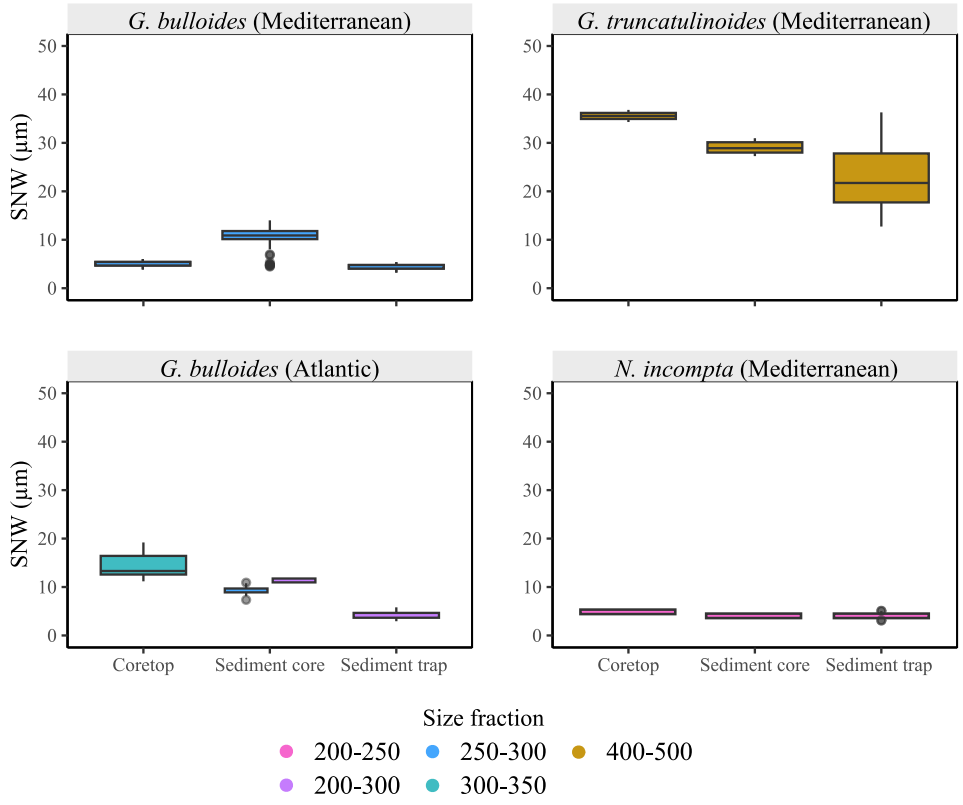

Figure S11 Boxplot showing the weight of foraminifers under different sampling methods for *G. bulloides, G. truncatulinoides* and *N. incompta* in the Mediterranean and the Atlantic. The data has been split in this way to remove the impact of size fraction, species, and location, which enables direct comparisons between sampling methods from the raw SNW data.

Table S1. Breakdown of CMIP6 models used to extract environmental data. All models include a "historical" simulation with forcing terms following their historical records (1850–2010), and a "piControl" with steady preindustrial forcing. "pi" is short for preindustrial control or PiControl. TEOS is short for the International Thermodynamic Equation of Seawater (TEOS-10). We only used data which was regridded (.gr) and not natural gridded (.gn). A tick mark [✓] indicates which model is used. n/a is where data is not available on the ESGF (Earth System Grid Federation).
[1] The Jiang model output uses the median values from all models listed in the table, which has been processed as per the methods in Jiang et al (2023).
[2] The Jiang model output was for the open-ocean, therefore did not contain data for the Mediterranean. The biogeochemistry output for the CEMS2 model was the closest match to the median biogeochemistry of the 14 model ensemble, hence CESM2 was used to extract carbonate system, temperature and salinity data for the Mediterranean.

Model	Variant	pi start point	Density factor (kg/m3)	Carbonate system, salinity & temperature	Phosphate	Chlorophyll	Net primary productivity
Jiang Model output[1]	-	-	-	✓[2]	-	-	
ACCESSESM1-5	r1i1p1f1	161	1024.5	-	.gn	.gn	.gn
CESM2	r11i1p1f1	601	TEOS	-	✓	✓	✓
CMCC-ESM2	r1i1p1f1	1850	TEOS	-	.gn	.gn	.gn
CNRM-ESM-2	r1i1p1f2	1850	TEOS	-	.gn	.gn	.gn
GFDL-CM4	r1i1p1f1	151	1035	-	✓	✓	✓
GFDL-ESM4	r1i1p1f1	101	1035	-	✓	✓	✓
IPSL- CM6ALR	r1i1p1f1	1910	1028	-	.gn	.gn	.gn
MIROC-ES2L	r1i1p1f2	1850	TEOS	-	✓	✓	✓
MPI-ESM1-2- LR	r1i1p1f1	1850	1025	-	.gn	.gn	.gn
MRI-ESM2-0	r1i2p1f1	1850	1024.5	-	✓	✓	✓
CanESM5	r1i1p1f1	5201	1025	-	n/a	.gn	.gn
NorESM2-LM	r1i1p1f1	1600	TEOS	-	n/a	n/a	n/a
UKESM1-0-LL	r1i1p1f2	2250	TEOS	-	n/a	n/a	.gn
EC-Earth3-CC	r1i1p1f1	1850	TEOS	-	n/a	n/a	n/a

Table S2. Extended version of table 2. Compilation of previous studies assessing the relationship between planktonic foraminiferal size-normalized weight (SNW) and the environment. + = positive correlation, − = negative correlation, ~ = no response, a = Not specifically tested, only implied, b = Variable measured at the sea surface, c = Depth not explicitly stated. This table summarizes information from measurement based SNW (i.e. silhouette area [ρA], or diameter normalised) studies only and omits those which only normalised to size by sieving (i.e. sieve-based weights; SBW) or use plankton tow data. [1] Barker & Elderfield (2002); [2] Béjard et al. (2023); [3] Marr et al. (2011); [4] Marshall et al. (2013); [5] Osborne et al. (2016); [6] Pallacks et al. (2023); [7] Weinkauf et al. (2016).

Species	Data type	SNW measurement type	Symbiont	Spinose	Carbonate ion	pH	CO2	Temperature	Productivity	Phosphate	Nitrate	Salinity	Optimum conditions
symbiont-barren, spinose													
G. bulloides[6]	Core	MBW, diameter	Non-Symbiont	Spinose	+ b		− b	− b					
G. bulloides[1]	Coretop	MBW, diameter	Non-Symbiont	Spinose	+ *b			~ ab					
G. bulloides[3]	Coretop	MBW, diameter	Non-Symbiont	Spinose				− c					
G. bulloides[5]	Trap/Core	MBW, ρA	Non-Symbiont	Spinose	+ c			~ c		~ c			
G. bulloides[2]	Trap	MBW, diameter	Non-Symbiont	Spinose	~ c	~ c	~ c	~ b	~ c	~ c	~ c	~ c	~
G. bulloides[7]	Trap	MBW, ρA	Non-Symbiont	Spinose	~ *c			~ b	~ b				−
symbiont-obligate, spinose													
G. elongatus[6]	Core	MBW, diameter	Symbiont	Spinose	+ b		− b	− b					
G. elongatus[7]	Trap	MBW, ρA	Symbiont	Spinose	~ c			+ b	− b				+

G. ruber[7]	Trap	MBW, ρA	Symbiont	Spinose	~ *c			+ b	– b			~
G. ruber[4]	Trap	MBW, ρA	Symbiont	Spinose	+ c			+ c				
G. sacculifer[4]	Trap	MBW, ρA	Symbiont	Spinose	+ c			+ c				
symbiont-barren, non-spinose												
G. inflata[1]	Coretop	MBW, diameter	Non-Symbiont	Non-Spinose	+ *ab			~ ab				
G. trunc[1]	Coretop	MBW, diameter	Non-Symbiont	Non-Spinose	+ *ab			~ ab				
G. trunc[2]	Trap	MBW, diameter	Non-Symbiont	Non-Spinose	+ c	~ c	~ c	+ b	– c	~ c	~ c	~ c	–
N. incompta[2]	Trap	MBW, diameter	Non-Symbiont	Non-Spinose	~c	~ c	~ c	+ b	~ c	~ c	~ c	~ c	~
N. pachyderma[1]	Coretop	MBW, diameter	Non-Symbiont	Non-Spinose	+ *ab			~ ab				

Table S3 Bayesian model structure, collinearity diagnostics (variance inflation factor; VIF and tolerance intervals, TI, and model fit. Environmental variables include sea surface carbonate ion concentration, phosphate concentration, salinity and net primary productivity (NPP). In the 'Group-level' Bayesian models, Environment and Sampling method were added as fixed effects, and Species was added as a random effect (intercept only). Sampling method can include data from coretop, sediment core and sediment trap. A VIF of ten or less and tolerance interval (TI) of > 0.1 indicates that collinearity is not problematic (Marcoulides & Raykov, 2019). [1]Models which use principal components (PCs) in place of individual environmental variables due to collinearity in the original data making dimensionality reduction necessary. Values for leave one out cross validation (LOO) are reported in $\widehat{\mathrm{elpd}}_{\mathrm{loo}}$ [± standard error]; a lower value indicates comparatively worse performance between the two models (e.g., null model performs worse than the full model).

		Model structure			Collinearity Diagnostics (VIF [TI])						Model fit		
Model name	***n***	**Environment**	**Sampling method**	**Species**	**Carbonate**	**Phosphate**	**NPP**	**Salinity**	**PC1**	**PC2**	**Bayes R2**	**Leave One Out Cross Validation (LOO)**	
Group-level models (i.e., foraminifera pooled together)													
"full model"	491	✓	✓	✓	1.08 [0.93]	1.08 [0.92]	1.45 [0.69]	1.03 [0.97]	-	-	90%	full model	0
												null model	-247.5 [19.4]
"null model"	491	✓	✓	-	1.07 [0.94]	1.09 [0.92]	2.77 [0.36]	1.04 [0.96]	-	-	60%	null model	0
												env. only model	-114.4 [23.7]
"environment only"	491	✓	-	-	1.03 [0.97]	1.06 [0.95]	1.10 [0.91]	1.04 [0.96]	-	-	20%	-	
Species-level models													
G. truncatulinoides	105	✓[1]	✓	-	-	-	-	-	4.37 [0.23]	-	33%	-	
N. pachyderma	53	✓	-	-	3.63 [0.28]	3.71 [0.27]	4.28 [0.23]	3.66 [0.27]	-	-	55%	-	
G. elongatus	134	✓[1]	✓	-	-	-	-	-	1.15 [0.87]	1.98 [0.51]	88%	-	
G. ruber	53	✓	✓	-	4.99 [0.20]	1.85 [0.54]	3.55 [0.28]	3.49 [0.29]	-	-	78%	-	
G. bulloides	255	✓	✓	-	3.73 [0.27]	4.34 [0.23]	2.81 [0.36]	3.88 [0.26]	-	-	65%	-	
N. incompta	85	✓[1]	✓	-	-	-	-	-	3.48 [0.29]	1.63 [0.61]	78%	-	
G. truncatulinoides coretop 0m	40	✓	-	-	1.12 [0.89]	-	1.04 [0.96]	1.17 [0.86]	-	-	34%	-	
G. truncatulinoides coretop 200m	40	✓	-	-	4.16 [0.24]	-	2.46 [0.41]	2.41 [0.41]	-	-	54%	-	

Table S4. Effect size and 95% credible interval [lower, upper] for the association between SNW and the environment, from group-level (i.e. across species) and species-level Bayesian modelling for species that did not require PCA. See S2 and Table 3 in the main text for Bayesian model results of species that required PCA. If the credible interval crosses zero, there is a <95% probability that there is an effect. Colour indicates a positive or negative result. Note that the modelled dataset is slightly different between the group-level model and the species-level models. The group-level model dataset includes species which were omitted from species-level models due to their low sample size, and the size fraction ranges are more restricted for the group-level model due to a bias against larger size fractions in cooler environments (see methods).

Model	Carbonate	Phosphate	Salinity	NPP
Group-level	0.04 [0.01, 0.06]	−0.08 [−0.11, −0.06]	−0.02 [−0.06, 0.01]	0.01 [−0.00, 0.03]
G. bulloides	0.04 [−0.01, 0.09]	0.03 [−0.01, 0.08]	0.02 [−0.03, 0.07]	0.12 [0.05, 0.19]
G. ruber	0.33 [0.09, 0.58]	0.09 [−0.11, 0.30]	−1.14 [−1.35, −0.93]	−0.07 [−0.14, 0.00]
N. pachyderma	0.22 [0.14, 0.30]	0.05 [−0.05, 0.15]	−0.30 [−0.44, −0.16]	0.09 [0.02, 0.16]

S2. Principal component analysis (PCA)

For species *G. truncatulinoides, G. elongatus* and *N. incompta* collinearity was problematic (variance inflation factor (VIF) score was over ten; Marcoulides and Raykov, 2019). As such, to remove collinearity we reduce the dimensionality of the data with PCA and use the principal component outputs instead of individual environmental drivers in the Bayesian models. For these three species the PCA is based on the same four environmental drivers as all other modelling; carbonate ion concentration, phosphate concentration, net primary productivity (NPP), and salinity. These data were centred and scaled prior to PCA to ensure that environmental data were normalised.

G. truncatulinoides

Over half the of the variance in the environmental data is represented by principal component 1 (PC1; 59%; Table S5). Although including PC2 would increase the explained variance, its inclusion leads to multicollinearity in the resulting Bayesian model. As such, we only use PC1 for *G. truncatulinoides.* For this species, PC1 is primarily characterized by high loadings on salinity and phosphate (34% and 29% of the variance contribution respectively; Table S5), while carbonate contributes 20% and NPP 17%. PC1 score increase with salinity (i.e., positive loading) and decreases with higher values of phosphate, carbonate and NPP (i.e., negative loadings; Table S5; Fig. S12).

G. elongatus

Together, PC1 and PC2 explain 88% of the variance in environmental data for *G. elongatus* (Table S5). PC1 is primarily characterized by phosphate, NPP and salinity (34%, 34% and 27%, respectively), while PC2 is primarily characterized by carbonate ion concentration (80%). PC1 scores increase with phosphate and carbonate ion concentration, but decreases with salinity and NPP (Table S5; Fig. S12). PC2 is most strongly associated with a decrease in carbonate ion concentration but also shows negative loadings for salinity, phosphate, and NPP.

N. incompta

For *N. incompta*, PC1 and PC2 together explain 98% of the variance in the environmental data (Table S5). PC1 is characterized by relatively balanced loadings across the four environmental variables, with slightly higher loadings for salinity (29%) and phosphate (28%). In contrast, PC2 is primarily associated with NPP and carbonate, with loadings of 60% and 39%, respectively. PC1 scores increase with phosphate and decrease with higher salinity, carbonate, and NPP. PC2 scores increase with NPP and decrease with carbonate (Table S5; Fig. S12).

Table S5 Results from Principal Component Analysis for *G. truncatulinoides, G. elongatus* and *N. incompta.* Eigenvalue and variance explained (%) indicate how well the principal component explains the environmental data. Squared cosines (cos^2) and percentage contribution show how well a particular environmental variable is represented in the principal component. Loadings (Eigenvectors) are indicative of the correlation between variables.

	Eigenvalue	**Variance explained (%)**	**Quality of representation of variable; cos^2 [percent contribution]**				**Variable loadings (Eigenvectors)**			
			Salinity	**PO_4**	**Carbonate**	**NPP**	**Salinity**	**PO_4**	**Carbonate**	**NPP**
G. truncatulinoides										
PC1	2.37	59.31	0.81 [34.11%]	0.68 [28.55%]	0.48 [20.34%]	0.40 [16.99%]	0.58	-0.54	-0.45	-0.41
G. elongatus										
PC1	2.47	61.67	0.66 [26.84%]	0.84 [34.44%]	0.12 [5.03%]	0.83 [33.68%]	-0.52	0.59	0.22	-0.58
PC2	1.04	26.11	0.16 [15.22%]	0.02 [2.31%]	0.84 [80.17%]	0.02 [2.29%]	-0.39	-0.15	-0.90	-0.15
N. incompta										
PC1	3.42	85.47	0.98 [28.58%]	0.97 [28.43]	0.78 [22.75%]	0.69 [20.24%]	-0.53	0.53	-0.48	-0.45
PC2	0.48	12.05	0.00 [0.68%]	0.00 [0.01%]	0.18 [39.01%]	0.29 [60.28%]	-0.08	0.01	-0.62	0.78

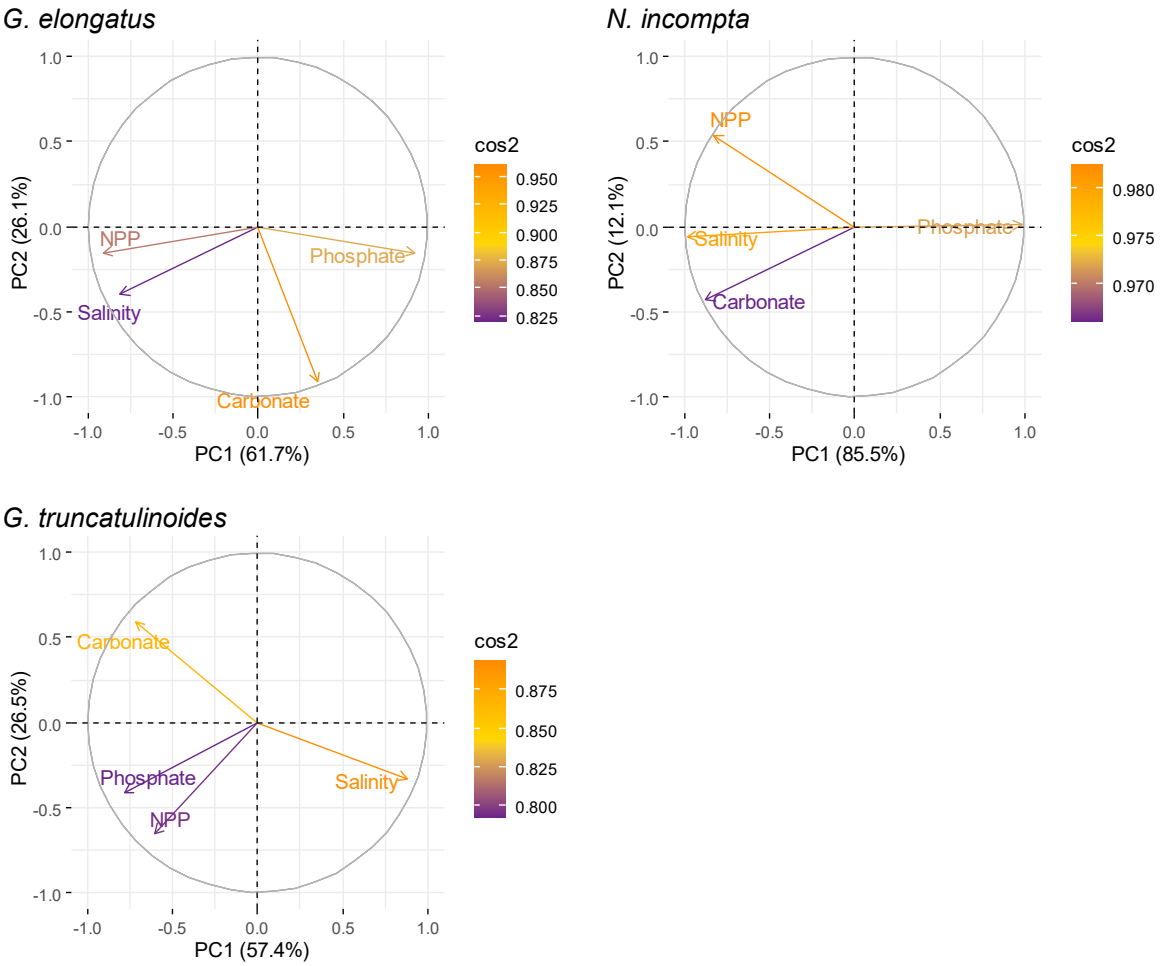

Figure S12 – Biplot outputs from principal component analysis for *G. truncatulinoides, G. elongatus* and *N. incompta* for principal component (PC) 1 and PC2 for each species. The percentage presented in each axis label is the Eigenvalue expressed as percentage (i.e., how much variance in the data is explained by that component). Squared cosine values (cos^2) are indicative of the strength of each variable's association with a principal component; the higher the value the better represented the variable is in that PC. The direction of the arrow along the axis describes the correlation between variables; positively correlated variables point to the same side of the plot and negatively correlated variables point to opposite sides of the graph.

S3. Additional analyses for depth of environmental variables

In the main text we use sea surface (≤ 20 m) environmental data in the Bayesian models, including for species that are generally deeper dwelling, e.g., *G. truncatulinoides.* As described in the main text, this is in part due to the challenge of estimating exact habitat depth for each specimen. Here we explore the importance of the depth of environmental data by performing further analyses using 200m depth environmental data from CESM2. We aimed to compare the model performance of two *G. truncatulinoides* models, one analysed with deeper (200m) environmental data and one with shallower (≤ 20 m) environmental data. As collinearity was present in the datasets (VIF >10) it was necessary either (a) reduce the dimensionality of data with principal component analysis (PCA), or because collinearity is primarily associated with sampling method in *G. truncatulinoides*, (b) model coretop data and sediment trap data separately. Because we wanted to compare the models, PCA would have been inappropriate as it would result in differing principal components for the models. Hence, we take option two and for *G. truncatulinoides*, model coretop data and sediment trap data separately. For each we run a sea surface (≤ 20m) environmental data model and a deep (200m) environmental data model. The sediment trap data models had to be abandoned due to excessive collinearity (VIF >10). Phosphate was removed from both coretop data models due to collinearity (VIF >10), leaving carbonate ion concentration, net primary productivity (NPP) and salinity.

The explained variance of coretop *G. truncatulinoides* was higher in the 200m depth model than in the sea surface model (Bayes R2 54% and 34%, respectively; Table S3) showing an improvement of the link between SNW and environment for the deeper data. It is important to note that while there is a comparative improvement in model performance with the 200m depth data, still only half of SNW is explained by these three environmental variables leaving large uncertainties about other drivers for SNW in this species. We are hesitant to overinterpret these models due to the fairly low explained variance and small sample size (n = 40), however the overlap of the 95% credibility intervals for coefficient estimates (Fig. S13) suggest little difference between models. The low explained variance in SNW for these models, and for all *G. truncatulinoides* analysed using PCA (33% Table S3), might be related to the much longer life time of this species meaning that it experiences a wide range of environmental conditions given the vast distances this taxon drifts during its lifetime (van Sebille et al., 2015; Waterson et al., 2017).

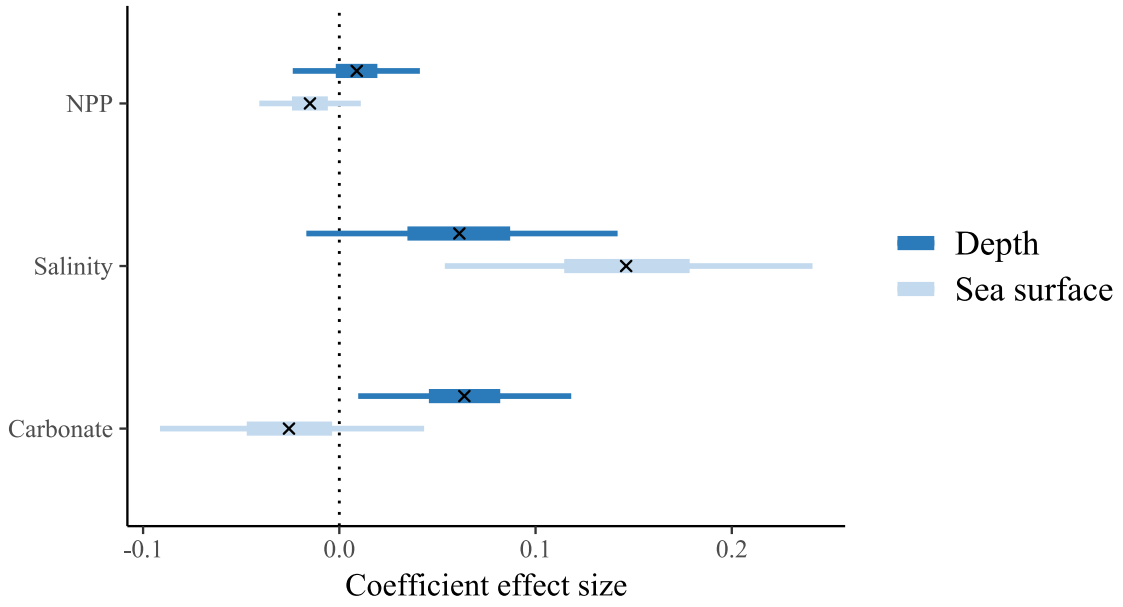

Figure S13 Effect size and credible intervals for the association between SNW and the environment for a *G. truncatulinoides* model using sea surface data (20m or less) and a model using deeper data (200m). A cross [x] represents the median value, the thicker line the 50% interval (i.e., where 50% of the posterior probability lies) and the thinner line the 95% interval. If the 95% interval does not cross zero, then there is a 95% probability there is an effect of the environmental variable. A negative value represents a negative correlation between SNW and the coefficient.

Barker, S.: Planktonic foraminiferal proxies for temperature and pCO2, Ph.D. thesis, University of Cambridge, England, 2002.

Barker, S. and Elderfield, H.: Foraminiferal calcification response to glacial-interglacial changes in atmospheric CO2, Science, 297, 833–836, https://doi.org/10.1126/science.1072815, 2002.

Barrett, R.: Planktic foraminifera size-normalised weight data and associated environmental data [dataset bundled publication]., https://doi.org/https://doi.org/10.1594/PANGAEA.973256, 2025.

Béjard, T. M., Rigual-Hernández, A. S., Flores, J. A., Tarruella, J. P., Durrieu De Madron, X., Cacho, I., Haghipour, N., Hunter, A., and Sierro, F. J.: Calcification response of planktic foraminifera to environmental change in the western Mediterranean Sea during the industrial era, Biogeosciences, 20, 1505–1528, https://doi.org/10.5194/BG-20-1505-2023, 2023.

van Heuven, S., Pierrot, D., Rae, J. W. B., Lewis, E., and Wallace, D. W. R.: MATLAB Program Developed for CO2 System Calculations, https://doi.org/https://doi.org/10.3334/CDIAC/otg.CO2SYS_MATLAB_v1.1, 2011.

Jiang, L. Q., Dunne, J., Carter, B. R., Tjiputra, J. F., Terhaar, J., Sharp, J. D., Olsen, A., Alin, S., Bakker, D. C. E., Feely, R. A., Gattuso, J. P., Hogan, P., Ilyina, T., Lange, N., Lauvset, S. K., Lewis, E. R., Lovato, T., Palmieri, J., Santana-Falcón, Y., Schwinger, J., Séférian, R., Strand, G., Swart, N., Tanhua, T., Tsujino, H., Wanninkhof, R., Watanabe, M., Yamamoto, A., and Ziehn, T.: Global Surface Ocean Acidification Indicators From 1750 to 2100, J. Adv. Model. Earth Syst., 15, https://doi.org/10.1029/2022MS003563, 2023.

Marcoulides, K. M. and Raykov, T.: Evaluation of Variance Inflation Factors in Regression Models Using Latent Variable Modeling Methods, Educ. Psychol. Meas., 79, 874, https://doi.org/10.1177/0013164418817803, 2019.

Marr, J. P., Baker, J. A., Carter, L., Allan, A. S. R., Dunbar, G. B., and Bostock, H. C.: Ecological and temperature controls on Mg/Ca ratios of Globigerina bulloides from the southwest Pacific Ocean, Paleoceanography, 26, https://doi.org/10.1029/2010PA002059, 2011.

Marshall, B. J., Thunell, R. C., Henehan, M. J., Astor, Y., and Wejnert, K. E.: Planktonic foraminiferal area density as a proxy for carbonate ion concentration: A calibration study using the Cariaco Basin ocean time series, Paleoceanography, 28, 363–376, https://doi.org/10.1002/palo.20034, 2013.

McDougall, T. J. and Barker, P. M.: Getting started with TEOS-10 and the Gibbs seawater (GSW) oceanographic toolbox, https://www.teos-10.org/pubs/Getting_Started.pdf, 2011.

Osborne, E. B., Thunell, R. C., Marshall, B. J., Holm, J. A., Tappa, E. J., Benitez-Nelson, C., Cai, W. J., and Chen, B.: Calcification of the planktonic foraminifera Globigerina bulloides and carbonate ion concentration: Results from the Santa Barbara Basin, Paleoceanography, 31, 1083–1102, https://doi.org/10.1002/2016PA002933, 2016.

Pallacks, S., Ziveri, P., Schiebel, R., Vonhof, H., Rae, J. W. B., Littley, E., Garcia-Orellana, J., Langer, G., Grelaud, M., and Martrat, B.: Anthropogenic acidification of surface waters drives decreased biogenic calcification in the Mediterranean Sea, Commun. Earth Environ., 4, 1–10, https://doi.org/10.1038/s43247-023-00947-7, 2023.

Qin, B., Li, T., Xiong, Z., Algeo, T. J., and Chang, F.: Deepwater carbonate ion concentrations in the western tropical Pacific since 250 ka: Evidence for oceanic carbon storage and global climate influence, Paleoceanography, 32, 351–370, https://doi.org/10.1002/2016PA003039, 2017.

van Sebille, E., Scussolini, P., Durgadoo, J. V., Peeters, F. J. C., Biastoch, A., Weijer, W., Turney, C., Paris, C. B., and Zahn, R.: Ocean currents generate large footprints in marine palaeoclimate proxies, Nat. Commun., 6, 1–8, https://doi.org/10.1038/ncomms7521, 2015.

Waterson, A. M., Edgar, K. M., Schmidt, D. N., and Valdes, P. J.: Quantifying the stability of planktic foraminiferal physical niches between the Holocene and Last Glacial Maximum, Paleoceanography, 32, 74–89, https://doi.org/10.1002/2016PA002964, 2017.

Weinkauf, M. F. G., Kunze, J. G., Waniek, J. J., and Kučera, M.: Seasonal Variation in Shell Calcification of Planktonic Foraminifera in the NE Atlantic Reveals Species-Specific Response to Temperature, Productivity, and Optimum Growth Conditions, PLoS One, 11, e0148363, https://doi.org/10.1371/journal.pone.0148363, 2016.